

# Analiza kinematike toka v rotirajočem difuzorju

An Analysis of the Flow Kinematics in a Rotating Diffuser

Tom Bajcar · Brane Širok · Ferdinand Trenc · Dragica Jošt

V prispevku so predstavljene raziskave hitrostnega polja toka zraka v rotirajočem vzdolžnem difuzorju okroglega prereza. Meritve hitrostnih komponent toka so potekale z uporabo laser-Dopplerjeve anemometrije (LDA). Z meritvami je bila potrjena delitev toka na zunanjji vrtilni del ob vrteči se steni in notranji nevrtilni del v vzdolžni osi difuzorja. Ugotovljeno je bilo pomembno povečanje vseh treh komponent hitrosti v ozkem pasu ob vrteči se steni difuzorja. Poleg tega je bil izveden tudi numerični izračun hitrostnega polja v difuzorju s tremi različnimi turbulentnimi modeli.

© 2002 Strojniški vestnik. Vse pravice pridržane.

(Ključne besede: difuzorji rotirajoči, kinematika toka, polja hitrostna, anemometrija Dopplerjeva, anemometrija laserska)

This paper describes a study of the flow-velocity field inside a rotating axial diffuser with a circular cross-section. The flow-velocity components were measured with an LDA system. The velocity-component measurements confirmed the existence of two types of flow: a rotating region near the rotating wall and a non-rotating region near the longitudinal axis of the diffuser. A significant increase in all three velocity components was observed in a thin layer at the rotating-diffuser wall. In addition, three different turbulence-closure models were applied for the velocity-field prediction inside the rotating diffuser.

© 2002 Journal of Mechanical Engineering. All rights reserved.

(Keywords: rotating diffusers, flow kinematics, velocity fields, laser-Doppler anemometry)

## 0 UVOD

Analiza hitrostnega polja turbulentnega toka tekočine v vrtečem se vzdolžnem difuzorju ima svoje osnove v raziskavah toka tekočine skozi difuzor in preučevanju vrtinčnih tokov. Začetek pomembnejših raziskav toka v difuzorju sega nekako v prva desetletja 20. stoletja, predvsem z namenom preučiti dogajanje v mejni plasti difuzorja pri različnih kotih razširitve difuzorja [1]. Preveliki koti razširitve namreč povzročijo, da se mejna plast ob steni difuzorja na določenem mestu odlepi od stene, kar je posledica vzdolžnih tlačnih gradientov.

Ena izmed glavnih značilnosti vrtinčnih tokov je pojav centrifugalne sile kot posledice radialnega tlačnega gradienca, ki se pojavi v vrtinčnih tokovih [2]. V najpreprostejši obliki z zanemaritvijo strižnih sil ima radialni tlačni gradient  $\partial p / \partial r$  obliko:

$$\frac{\partial p}{\partial r} = \rho \cdot \frac{u_t^2}{r} \quad (1),$$

kjer so:  $\rho$  gostota tekočine,  $u_t$  njegova obodna hitrost,  $r$  pa radij. Centrifugalna sila pospešuje širjenje curka vrtinčnega toka radialno navzven.

## 0 INTRODUCTION

Analyses of the velocity field of the turbulent fluid flow in an axially rotating diffuser are based on studies of the fluid flowing through a stationary diffuser and on investigations of the swirl flow. Studies of flow inside the diffuser were initiated in the first decades of the 20<sup>th</sup> century, mainly to investigate the fluid behaviour inside the diffuser's boundary layer at different diffuser cone angles [1]. Diffuser cone angles that are too large cause the boundary layer at a particular point of the diffuser to separate from the wall. This separation is a consequence of the axial pressure gradients.

One of the main properties of the swirl flow is the presence of a centrifugal force, which is a consequence of the radial pressure gradient in swirl flows [2]. The simplest form of the radial pressure gradient  $\partial p / \partial r$ , where the shear forces are negligible, can be expressed as:

$$\frac{\partial p}{\partial r} = \rho \cdot \frac{u_t^2}{r} \quad (1),$$

where  $\rho$ ,  $u_t$  and  $r$  denote fluid density, fluid tangential velocity and radius, respectively. The centrifugal force enhances the swirling flow jet to spread radially outwards.

Raziskave turbulentnih vrtinčnih tokov, ki nastanejo v osno rotirajočih ravnih cevih [3], so pokazale predvsem povečanje obodnih in radialnih komponent hitrosti tekočine v bližini vrteče se stene cevi, profili vzdolžne komponente hitrosti tekočine pa so po obliku postali bolj podobni laminarnim kakor turbulentnim (t.i. laminarizacija). Poleg tega je bilo ugotovljeno tudi zmanjšanje hidravličnih izgub v primerjavi z mirujočo cevjo.

Očitno je, da toka skozi vrtečo se cev ni mogoče povsem primerjati s tokom skozi vrteči se difuzor, saj je treba pri slednjem upoštevati geometrijsko obliko difuzorja, ki povzroči mnoge kakovostne in količinske spremembe v toku, še posebej v njegovi mejni plasti oz. v plasteh tekočine tik ob steni difuzorja. Raziskave vrtinčnega toka v vzdolžnih difuzorjih okroglega prerezja so redke; ena izmed izčrpnejših je študija Clausena in sod. [4], ki predstavlja raziskavo vrtinčnega toka iz vrteče se cevi, katerega vrtinec prepreči odlepljanje mejne plasti od stene mirujočega difuzorja s kotom razširitve  $20^\circ$ .

Rezultati tu predstavljenega preskusa so v nadaljevanju pogosto primerjani z ugotovitvami zgoraj navedenih raziskav.

## 1 OPIS PRESKUSA

Analiza hitrostnega polja v difuzorju je bila izvedena na merilni postaji, ki jo prikazuje slika 1. Postavljena je bila v Laboratoriju za toplotne batne stroje na Fakulteti za strojništvo v Ljubljani. Difuzor, katerega shema je na sliki 2, je bil izdelan iz pleksi stekla in je bil prek jeklene zunanjne cevi in ležajev povezan z notranjo mirujočo cevjo. Geometrijske karakteristike difuzorja so naslednje: dolžina stožastega dela  $L = 165$  mm, kot razširitve oz. razširitve  $\theta = 18^\circ$ , vstopni premer  $d_v = 60$  mm, razmerje izstopnega in vstopnega prereza  $A_{iz}/A_v = 3.5$ .

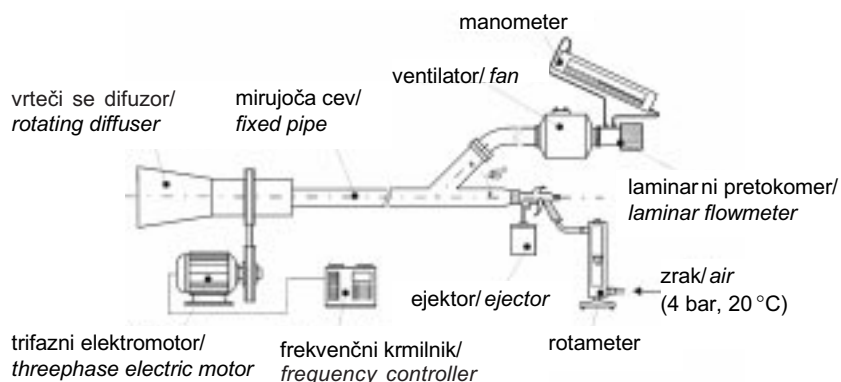
Studies of swirl flows in axially rotating straight pipes [3] reported increased tangential and radial velocity components in the vicinity of the rotating-pipe wall, whereas the shape of the axial velocity-component profiles of the fluid became closer to the laminar profiles rather than the turbulent ones (the so-called "laminarization"). The reduction of hydraulic losses in comparison with a stationary pipe was revealed as well.

It is obvious that the swirl flow in an axially rotating straight pipe cannot be simply approximated by the swirl flow in a rotating diffuser; the geometrical properties of the latter cause many qualitative and quantitative changes in the flow, particularly in its boundary layer, that is in the fluid layers directly at the diffuser wall. There are only a few studies of the turbulent swirl flow in axial diffusers with a circular transverse section; one of the most comprehensive was published by Clausen et al. [4], who investigated the swirl flow (originating from an axially rotating pipe), which prevented the separation of the flow from the wall of a stationary axial diffuser with a cone angle of  $20^\circ$ .

The results of the experimental investigations presented in this paper were compared to appropriate results from other authors.

## 1 EXPERIMENTAL SET-UP

The analysis of the velocity field in the rotating diffuser was carried out on the experimental set-up shown in Fig. 1. The experimental set-up was located in the Laboratory for Reciprocating Engines at the Faculty of Mechanical Engineering in Ljubljana. The diffuser, shown in schematic view in Fig. 2, was made of Plexiglas and was fastened through the steel connection outer pipe and bearings to the non-rotating inner pipe. The diffuser has the following geometric characteristics: length of the conical part of the diffuser  $L = 165$  mm, cone angle  $\theta = 18^\circ$ , inlet diffuser diameter  $d_v = 60$  mm, diffuser outlet-to-inlet area ratio  $A_{iz}/A_v = 3.5$ .



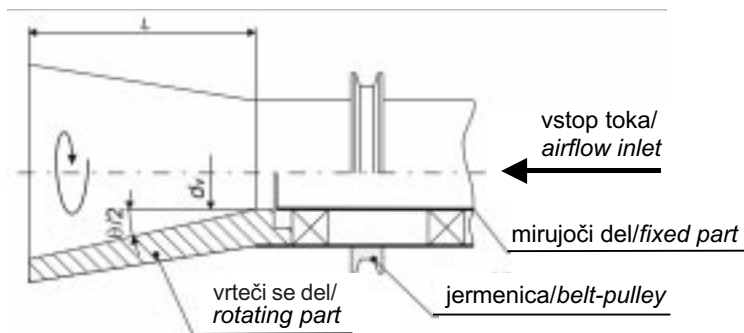
Sl. 1. Shema merilne postaje  
Fig. 1. Schematic view of the experimental station

Difuzor se je vrtel okrog svoje vzdolžne osi prek jermenice z uporabo dvopolnega trofaznega elektromotorja SEVER z močjo 1,5 kW pri  $2810 \text{ min}^{-1}$ . Elektromotor je bil krmiljen z vektorskim frekvenčnim pretvornikom MITSUBISHI FREQROL-A024, s katerim se je lahko spreminala vrtlina frekvenca elektromotorja in s tem tudi difuzorja. Na koncu mirujoče cevi dolžine 1900 mm, ki je vodila k difuzorju, je bil pritrjen ejektor, ki je služil kot generator delcev oziroma vir pasivnega onesnaževala, potrebnega za vizualizacijo toka ter merjenje hitrostnih profilov z metodo LDA. Kemična sestava kapljic onesnaževala je bila 80 prostorninskih % vode in 20 prostorninskih % zelo goste tekočine za meglo (tip E) proizvajalca Conrad Electronic. Ejekcija kapljic je bila izvedena s stisnjениm zrakom z nadtlakom 4 bar, ki je tekel skozi rotameter HEINRICHS 237929, kar je v mirujoči cevi vzpostavilo prostorninski tok  $\dot{V} = 4 \text{ l/s}$ . Z uporabo vzdolžnega ventilatorja in njegovega napetostnega krmilnika se je prostorninski tok v mirujoči cevi lahko povečal. Prostorninski tok zraka skozi ventilator je bil merjen z laminarnim pretokomerom MERIAM Instruments – Laminar Flow Element Model 50MC2-2f. Tok zraka je iz ventilatorja vstopal v mirujočo cev pod kotom  $45^\circ$ . Difuzor je deloval pri treh različnih vrtlinskih frekvencah  $f$  in treh različnih prostorninskih tokovih zraka  $\dot{V}$  oziroma vrednostih Reynoldsovega števila na vstopu v difuzor  $Re$  (preglednica 1).

Smer vrtenja difuzorja je bila pri obeh vrtlinskih frekvencah enaka, in sicer v nasprotni smeri urnega kazalca, opazovano od izstopa iz difuzorja proti njegovemu vstopu. Vse navedene vrednosti Reynoldsovega števila predstavljajo vrednosti Reynoldsovega števila na vstopu v difuzor.

The diffuser rotated around its longitudinal axis via a belt-pulley and was driven by a SEVER triphase electric motor with a power output of 1.5 kW at  $2810 \text{ min}^{-1}$ . A MITSUBISHI FREQROL-A024 vector frequency inverter was applied to alternate the rotating speed of the motor and thus the rotating frequency of the diffuser. An ejector was placed at the end of a 1900-mm-long fixed (non-rotating) pipe that led to the diffuser. The ejector was used as a particle generator that provided passive pollutant to the airflow for LDA measurements. The pollutant droplets consisted of 80 vol% of water and 20 vol% of very thick fog fluid (type E), distributed by Conrad Electronic. The droplets were ejected by pressurized air at 4 bar, flowing through a HEINRICHS 237929 rotameter. Thus, an axial airflow of  $\dot{V} = 4 \text{ l/s}$  entered the non-rotating pipe through the particle generator. The axial airflow through the diffuser could be increased by introducing additional airflow to the non-rotating pipe from a controlled fan. The volumetric airflow through the fan was measured with a MERIAM Instruments Laminar Flow Element, Model 50MC2-2f. The airflow from the fan entered the non-rotating pipe at an angle of  $45^\circ$ . The diffuser operated at three different rotating frequencies,  $f$ , as well as at three different volumetric airflows,  $\dot{V}$ , with the appropriate values of a diffuser-inlet Reynolds number  $Re$  (Table 1).

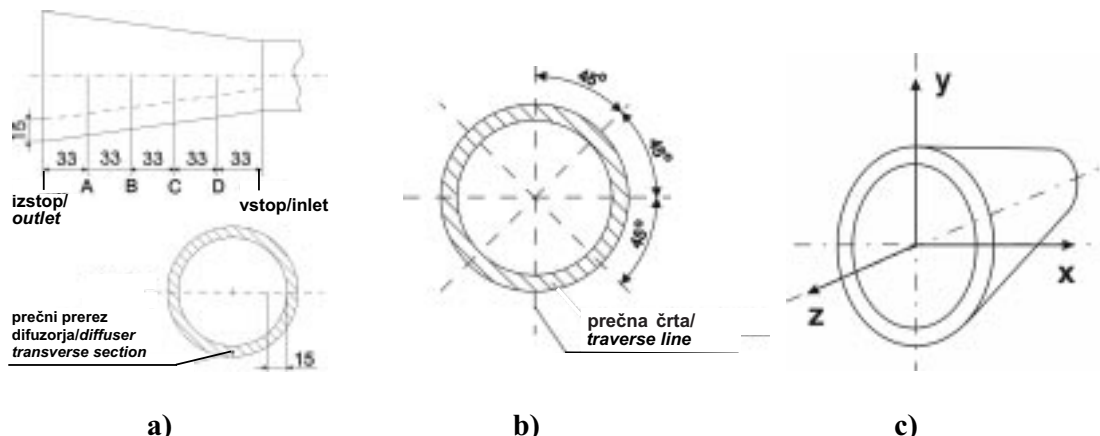
The direction of the diffuser rotation at both rotating frequencies was anti-clockwise when observed from the diffuser outlet towards its inlet. All reported values of the Reynolds number,  $Re$ , in the following text denote values of the diffuser-inlet Reynolds number.



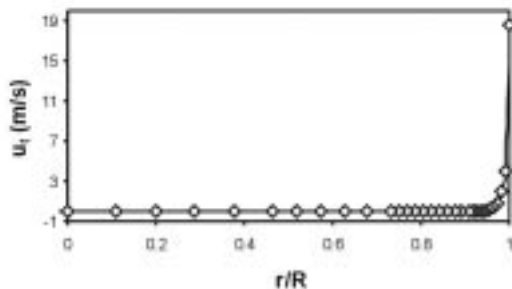
Sl. 2. Shema zgradbe rotirajočega difuzorja  
Fig. 2. Schematic view of the rotating diffuser

Preglednica 1. Vrtlne frekvence difuzorja, prostorninski tokovi in vrednosti vstopnega Reynoldsovega števila  
Table 1. Rotating frequencies of the diffuser; airflows and values of the inlet Reynolds number

$f$ Hz	$\dot{V}$ l/s	$Re$
0	4	$5,84 \cdot 10^3$
30	8	$1,17 \cdot 10^4$
52,8	13,8	$2,01 \cdot 10^4$



Sl. 3. a) – Merilna mesta znotraj difuzorja (mere v milimetrih); b) – Prečne črte na vstopnem in izstopnem prečnem prerezu difuzorja; c) – Uporabljeni koordinatni sistem  
 Fig. 3. a) – Positions of the measurement points inside the diffuser cone (all dimensions in millimetres); b) – Traverse lines in the diffuser inlet and outlet transverse section; c) - Coordinate system applied for measurements of velocity components



Sl. 4. Časovno povprečene srednje vrednosti obodne hitrosti  $u_t$  na izstopu iz difuzorja na x-osi koordinatnega sistema ( $f = 52,8 \text{ Hz}$ ,  $Re = 5,84 \times 10^3$ )  
 Fig. 4. Distribution of the time-averaged mean tangential velocity  $u_t$  at the diffuser outlet on the x-axis of the coordinate system ( $f = 52.8 \text{ Hz}$ ,  $Re = 5.84 \times 10^3$ )

Merjenje hitrostnih profilov s sistemom LDA je potekalo v vseh obratovalnih razmerah, in sicer v pasu 15 mm ob steni na štirih enako oddaljenih prečnih prerezih (A, B, C in D) v notranjosti difuzorja (sl. 3a), poleg tega pa tudi na vstopnem in izstopnem prerezu difuzorja na štirih prečnih črtah (sl. 3b). Slika 3c prikazuje uporabljeni koordinatni sistem. Razmerje  $r/R$  na diagramih predstavlja razmerje oddaljenosti merilnega mesta od vzdolžne osi difuzorja  $r$  s polmerom tekočega prečnega prereza difuzorja  $R$ .

Measurements of the velocity components with the LDA system were carried out for all the aforementioned operating conditions in a 15-mm-wide band directly at the diffuser wall in four equidistant transverse sections (A, B, C and D) inside the diffuser (Fig. 3a). Apart from that, the velocity components were also measured at the inlet- and outlet-difusser transverse sections on four traverse lines (Fig. 3b). The Cartesian coordinate system shown in Fig. 3c was used throughout the experiment. The expression  $r/R$  on the diagrams denotes the ratio between the radial distance of the measuring point from the diffuser longitudinal axis,  $r$ , and the radius of the particular diffuser transverse section,  $R$ .

## 2 REZULTATI

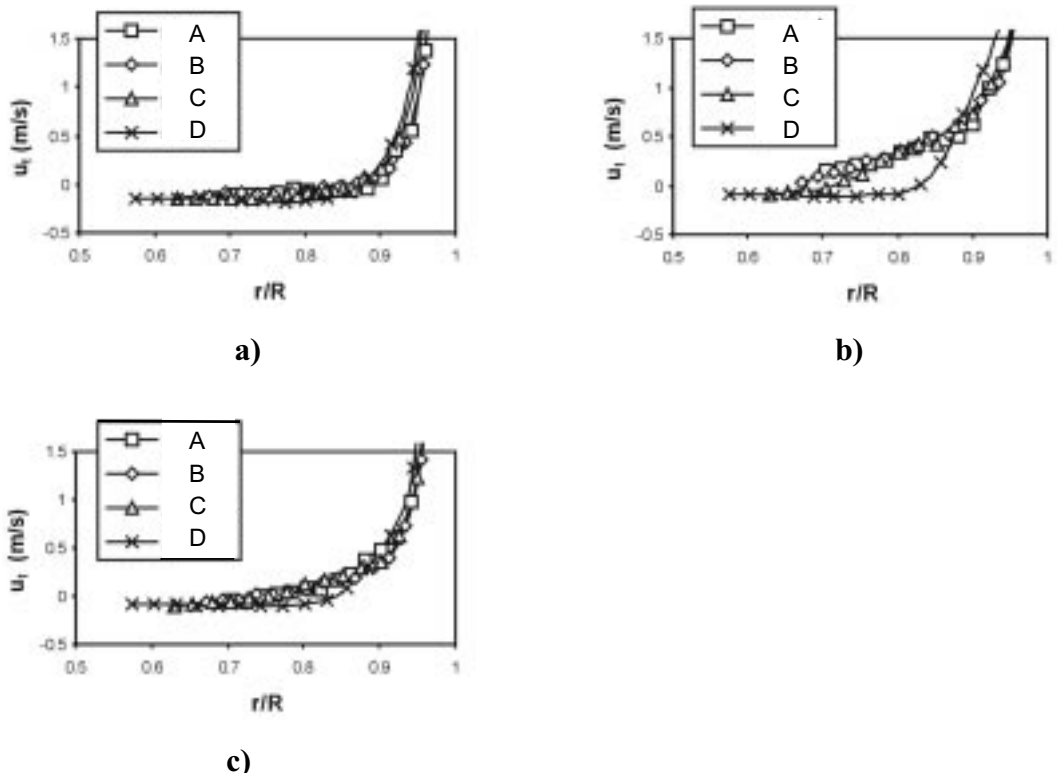
### 2.1 Potek časovno povprečenih srednjih vrednosti obodnih komponent hitrosti ( $u_t$ )

Vrtenje difuzorja okoli njegove vzdolžne osi povzroči v toku zraka obodne komponente hitrosti, saj plasti zraka ob notranji steni difuzorja sledijo vrtenju stene. S tem se v ravni x-y difuzorja pojavi vrtinec (sl. 4).

## 2 RESULTS

### 2.1 Distribution of time-averaged mean tangential velocity components ( $u_t$ )

Rotation of the diffuser around its longitudinal axis generates tangential velocity components because the layers of air at the inner diffuser wall follow the wall rotation. As a consequence a vortex appears in the x-y plane of the diffuser (Fig. 4).



Sl. 5. Časovno povprečene obodne komponente hitrosti na prečnih prerezih difuzorja A, B, C in D;  
a) –  $f = 30 \text{ Hz}$ ,  $\text{Re} = 1,17 \times 10^4$ ; b) –  $f = 30 \text{ Hz}$ ,  $\text{Re} = 2,01 \times 10^4$ ; c) –  $f = 52,8 \text{ Hz}$ ,  $\text{Re} = 2,01 \times 10^4$

Fig. 5. Distribution of the time-averaged mean tangential velocity components on diffuser transverse sections A, B, C and D; a) –  $f = 30 \text{ Hz}$ ,  $\text{Re} = 1.17 \times 10^4$ ; b) –  $f = 30 \text{ Hz}$ ,  $\text{Re} = 2.01 \times 10^4$ ; c) –  $f = 52.8 \text{ Hz}$ ,  $\text{Re} = 2.01 \times 10^4$

Slike 4 je razvidno, da se v difuzorju vrti ledel toka zraka v ozkem pasu ob vrteči se steni. Vrtilno območje je velikosti ~4 mm in obkroža nevrtilni del toka. Podoben pojav je bil opažen tudi v primeru vrtilne ravne cevi [5]. Oblika profilov obodnih komponent hitrosti se spreminja s spremenjanjem vrtinčnega razmerja  $N = u_{t,\text{stene}}/\bar{u}_a$ , ki predstavlja razmerje obodne hitrosti stene difuzorja in povprečne vzdolžne hitrosti zraka na izbranem prečnem prerezu difuzorja (sl. 5).

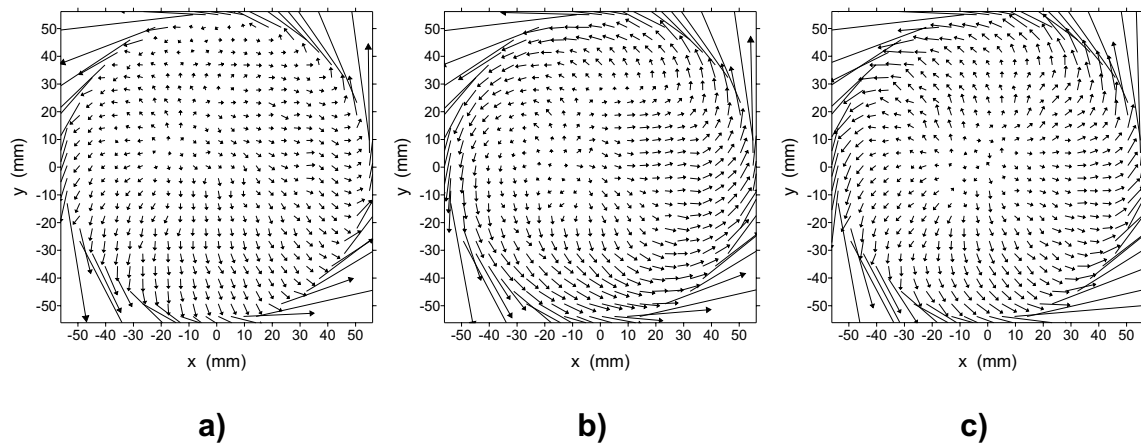
Slike 5 je razvidno, da se vpliv vrteče se stene na tok zraka v difuzorju poveča s povečevanjem prečnega premera difuzorja v smeri od vstopa proti izstopu difuzorja. Povečan vpliv vrteče se stene se kaže v širšem področju, kjer so obodne hitrosti zraka pozitivne oz. imajo isti predznak kot obodna hitrost stene difuzorja. Vrtinčno razmerje  $N$  je večje na prečnih prerezih, ki so bližje izstopu iz difuzorja (npr. prereza A in B), na teh prerezih pa je širše tudi območje pozitivnih obodnih hitrosti zraka.

Primerjava med slikama 5a in 5b pokaže, da je pri enakih vrtilnih frekvencah difuzorja in istih prečnih prerezih difuzorja vpliv vrteče se stene močnejši v primeru večjih vrednosti Reynoldsovega števila, torej pri manjšem razmerju  $N$ . Podoben pojav je opažen tudi v primeru, ko se pri enaki vrednosti Reynoldsovega števila zmanjša

It can be seen from Fig. 4 that only a small portion of the fluid inside the diffuser is rotating close to the diffuser wall. This region is about 4-mm wide and encircles the non-rotating core of the airflow. A similar phenomenon was also observed in the case of rotating straight pipes [5]. The shape of the tangential velocity profiles changes with the change of the swirl rate  $N = u_{t,\text{stene}}/\bar{u}_a$ , which represents the ratio between the diffuser-wall tangential velocity and averaged axial velocity of the air at a chosen diffuser transverse section (Fig. 5).

Fig. 5 shows that the influence of the rotating diffuser wall on the airflow in the diffuser generally increases together with the increasing diffuser transverse section in the direction from diffuser inlet to its outlet. The increased influence of the rotating wall reveals itself by means of a broader region, where the tangential velocity components of the airflow are positive (thus having the same sign as the tangential velocity of the diffuser wall). The swirl rate  $N$  is higher near the rotating diffuser outlet (e.g. at transverse sections A and B), therefore the region of positive tangential velocity components of the airflow is broader in the transverse sections at the diffuser outlet.

A comparison between Fig. 5a and Fig. 5b shows that at the same rotating frequency of the diffuser the influence of the rotating diffuser wall on the airflow is larger at higher Reynolds number values and therefore at a lower swirl rate,  $N$ , observed in a particular diffuser transverse section. A similar phenomenon can be observed when at



Sl. 6. Diagrami hitrosti na izstopu iz difuzorja v ravni x-y: a) –  $f = 30 \text{ Hz}$ ,  $Re = 1.17 \times 10^4$ ; b) –  $f = 30 \text{ Hz}$ ,  $Re = 2.01 \times 10^4$ ; c) –  $f = 52.8 \text{ Hz}$ ,  $Re = 2.01 \times 10^4$

Fig. 6. Velocity diagrams in  $x$ - $y$  plane at the diffuser outlet: a) –  $f = 30 \text{ Hz}$ ,  $Re = 1.17 \times 10^4$ ; b) –  $f = 30 \text{ Hz}$ ,  $Re = 2.01 \times 10^4$ ; c) –  $f = 52.8 \text{ Hz}$ ,  $Re = 2.01 \times 10^4$

vrtilna frekvenca difuzorja in s tem razmerje  $N$  (sl. 5b, 5c). To potrdijo tudi hitrostni diagrami v ravni x-y na izstopu iz difuzorja (sl. 6).

## 2.2 Potek časovno povprečenih srednjih vrednosti radialnih komponent hitrosti ( $u_r$ )

V vrtečem se difuzorju se kot posledica radialnega tlačnega gradiента en. (1) pojavi radialna komponenta hitrosti zraka v smeri proti vrteči se steni difuzorja. Največje radialne komponente hitrosti se po pričakovanju pojavijo v območju največjih obodnih hitrosti, saj so le-te glavni vzrok za nastanek radialnih komponent (centrifugalna sila).

Na sliki 7 so prikazani diagrami radialnih komponent hitrosti v različnih delovnih razmerah difuzorja na njegovem izstopu.

Diagrama na sliki 7 kažeta, da se največje vrednosti radialne komponente hitrosti pojavijo tik ob steni difuzorja na oddaljenosti  $r/R \approx 0.99$ . Največje vrednosti obodne hitrosti se pojavijo sicer neposredno na vrteči se steni sami ( $r/R = 1$ ), vendar zaradi stene tam radialne komponente ni. Poleg tega je razvidna odvisnost poteka radialnih komponent hitrosti od frekvence vrtenja difuzorja ter (vzdoljnega) Reynoldsovega števila, torej od razmerja  $N$ . Pri višji frekvenci vrtenja difuzorja in nespremenjeni vrednosti Reynoldsovega števila (višji  $N$ ) se pojavijo večje vrednosti radialnih komponent hitrosti, kar lahko pričakujemo, saj so v tem primeru večje tudi obodne komponente hitrosti zraka. Po drugi strani pa se pri večjih vrednostih Reynoldsovega števila in nespremenjeni vrtilni frekvenci difuzorja (nižji  $N$ ) pojavijo nižje vrednosti radialnih komponent hitrosti zraka; z naraščanjem radialne oddaljenosti od stene difuzorja pa vrednosti radialnih hitrosti pri manjših vrednostih  $N$  postopoma preraštejo tiste pri večjih vrednostih  $N$ .

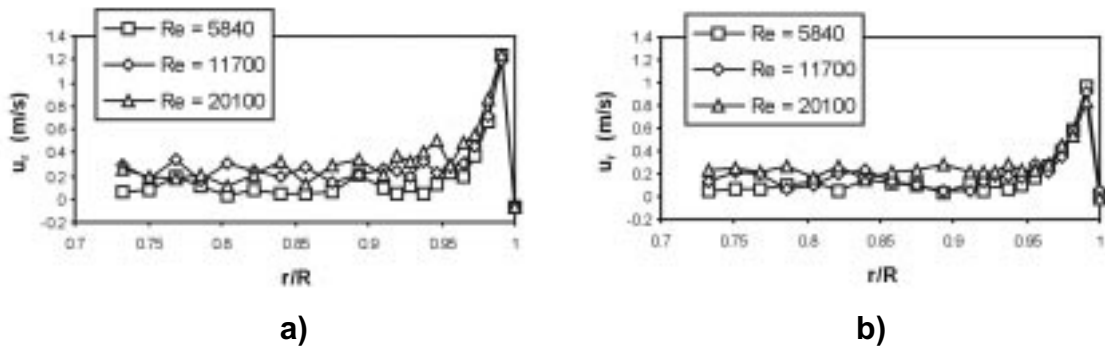
the same value of the Reynolds number the values the rotating frequency and thus the swirl rate,  $N$ , is reduced (Figs. 5b and 5c). This is also confirmed by velocity diagrams in the  $x$ - $y$  plane at the diffuser outlet (Fig. 6).

## 2.2 Distribution of time-averaged mean radial velocity components ( $u_r$ )

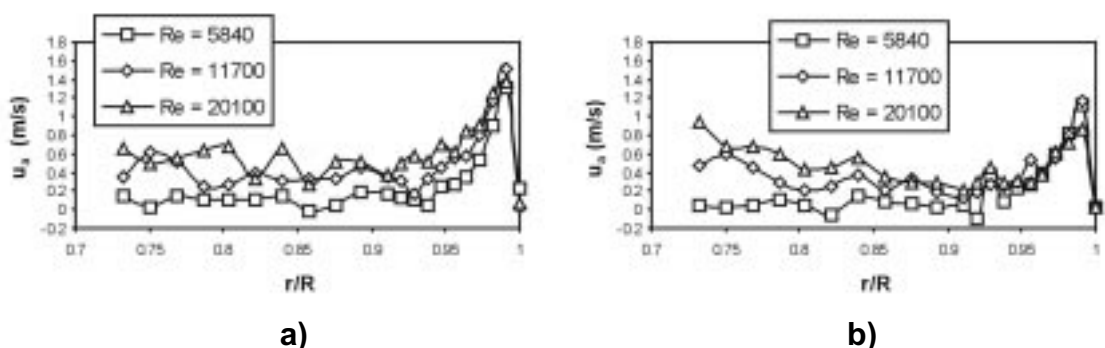
The radial velocity component in the airflow oriented towards the rotating diffuser wall appears in the rotating diffuser as a consequence of the radial pressure gradient (Eq.1). The peak radial velocities coincide with the region of the peak tangential velocities, as one would expect, since the tangential velocities are the main reason for the appearance of the radial velocities (centrifugal force).

Fig. 7 shows the diagrams of radial velocity components at the diffuser outlet at different operating conditions of the diffuser.

It can be clearly seen from the diagrams in Fig. 7 that the peak value of the radial velocity component occurs close to the wall in a rotating region of the airflow – at a relative distance of about  $r/R \approx 0.99$ . The highest values of the tangential velocity take place directly on the diffuser wall ( $r/R = 1$ ), but there is no radial component because of the wall. Apart from that, the radial velocity distribution depends on the rotating frequency of the diffuser and on the (axial) Reynolds number of the airflow, i.e. on the swirl rate  $N$ . A higher rotating frequency leads to higher radial velocity values at fixed values of  $Re$  (higher  $N$ ); this situation was anticipated because the peak tangential velocity values are also higher in this case. On the other hand, higher  $Re$  values at a fixed rotating frequency (lower  $N$ ) produce lower peak radial velocity component values; the values of the radial velocity at lower  $N$  eventually exceed those at higher  $N$  when the radial distance from the diffuser wall is increased.



Sl. 7. Potek časovno povprečenih radialnih komponent toku na izstopu iz difuzorja:

a) –  $f = 52,8 \text{ Hz}$ ; b) –  $f = 30 \text{ Hz}$ Fig. 7. Distribution of the time-averaged mean radial velocity components at the diffuser outlet:  
a) –  $f = 52.8 \text{ Hz}$ ; b) –  $f = 30 \text{ Hz}$ Sl. 8. Potek časovno povprečenih vzdolžnih komponent toku na izstopu iz difuzorja: a)  $f = 52,8 \text{ Hz}$ ; b)  $f = 30 \text{ Hz}$ Fig. 8. Distribution of the time-averaged mean axial velocity components at the diffuser outlet:  
a)  $f = 52.8 \text{ Hz}$ ; b)  $f = 30 \text{ Hz}$ 

### 2.3 Potek časovno povprečenih srednjih vrednosti vzdolžnih komponent hitrosti ( $u_a$ )

Na prečnih prerezih, ki so bliže izstopu iz difuzorja in kjer so obodne komponente hitrosti izrazitejše, se pojavi lokalni vrh vrednosti vzdolžnih hitrosti tik ob vrteči se steni difuzorja (sl. 8).

Povečanje vzdolžnih komponent tik ob steni ni bilo opaženo ne v primeru vrteče se ravne cevi [6], prav tako pa tudi ne v primeru vrtinčnega toka v mirujočem difuzorju [4]. Eden izmed vzrokov tega pojava leži v delovanju centrifugalne sile, ki potiska tok zraka proti steni difuzorja in s tem proti izstopu iz difuzorja (stena difuzorja se namreč razširja v smeri proti njegovemu izstopu). Drugi vzrok pa je čelna stena difuzorja oz. debelina stene difuzorja na njegovem izstopu; med vrtenjem difuzorja se zrak ob tej steni zaradi delovanja centrifugalne sile pomika v radialno-obodni smeri navzven v zunanji prostor [7], na njegovo mesto pa priteka nov zračni tok, ki ga čelna stena difuzorja "črpa" iz notranjosti difuzorja oziroma iz mejne plasti ob notranji steni difuzorja. Zaradi navedenih vzrokov ni med eksperimentom nikoli prišlo do odcepljanja plasti zraka tik ob notranji steni difuzorja (povratni tok), kljub temu, da je bil kot razširivite difuzorja večji od  $14^\circ$ .

### 2.3 Distribution of time-averaged mean axial velocity components ( $u_a$ )

There is a local peak of the axial velocities in the near-wall region in the transverse sections that are closer to the diffuser outlet and where the swirl is more intensive due to a higher wall tangential velocity (Fig. 8).

The increase in axial velocity component values near the diffuser wall has not been observed, neither in the case of the axially rotating straight pipes [6] nor in the case of the stationary diffuser with swirl flow [4]. One of the reasons for this phenomenon is in the action of the centrifugal force, which propels the airflow towards the diffuser wall and thus towards the diffuser outlet (since the diffuser cone diverges in the direction of its outlet). The second reason is the diffuser endplate – the thickness of the wall at the diffuser outlet. When the diffuser rotates, due to the centrifugal forces the air attached to this endplate is pushed out of the diffuser in the radially tangential direction [7]. Thus, the additional airflow is sucked in from the inner side of the diffuser cone (from the boundary layer at the inner diffuser wall) by the endplate. As consequence of the described phenomena, flow separation from the rotating diffuser wall (the so-called reverse flow) was never observed during the experiments, although the diffuser cone angle exceeded  $14^\circ$ .

Iz slike 8 je tudi razvidno, da je potek vzdolžnih komponent hitrosti zraka ob steni difuzorja podoben poteku radialnih komponent hitrosti v istem območju difuzorja (sl. 7).

#### 2.4 Rezultati numeričnih modelov

Numerični izračun toka zraka v vrtečem se difuzorju je potekal z uporabo CFD programskega paketa CFX-TASCflow, verzija 2.10. Pri tem so bili uporabljeni trije turbulentni modeli, ki so že vsebovani v omenjenem programskem paketu: model  $k-\varepsilon$ , model  $k-\omega SST$  in model Reynoldsovih napetosti. Vstopni in robni pogoji so bili za vse tri modele podani z eksperimentalnimi meritvami, s katerimi so bile določene časovno povprečene hitrostne komponente toka zraka na vstopu v difuzor. Na sliki 9 je prikazano območje okrog difuzorja (okolica, robni pogoji), ki je bilo uporabljeno pri modeliranju.

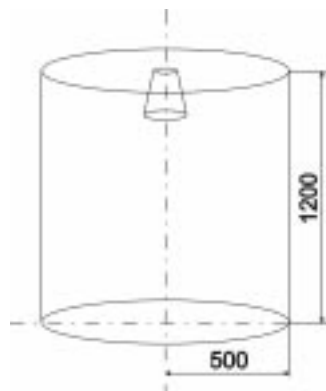
Rezultati numeričnih modelov in primerjava z eksperimentalno dobljenimi vrednostmi so prikazani na sliki 10.

It is obvious from Fig. 8 that the axial velocity distribution in the near-wall region of the airflow in the rotating diffuser is analogous to the distribution of radial velocities in the same region of the diffuser (Fig. 7).

#### 2.4 Results of the numerical models

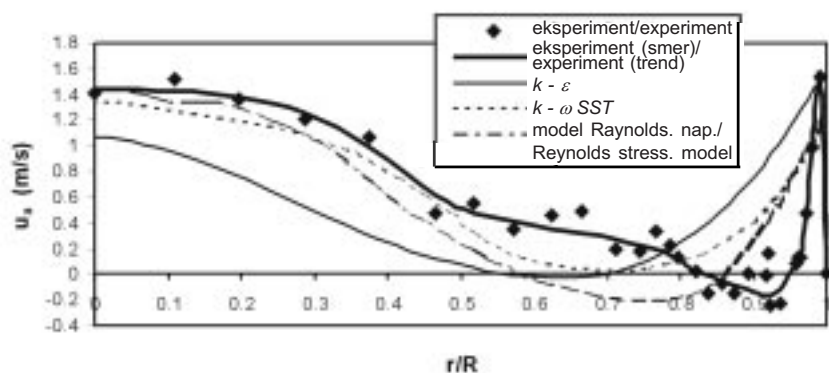
Numerical calculation of the airflow inside the rotating diffuser was carried out using a CFD program package: CFX-TASCflow, version 2.10. Three different turbulent closure models were used, which were already included in the aforementioned program package: the  $k-\varepsilon$  model, the  $k-\omega SST$  model and the Reynolds stresses model. The inlet and the boundary conditions for all three models were determined with experimental measurements, which were used for the calculation of the time-averaged velocity components of the airflow at the diffuser inlet. A region around the diffuser (surrounding, boundary conditions) used for modelling is shown in Fig. 9.

The results of the numerical models and the comparison with the experimentally acquired values are shown in Fig. 10.



Sl. 9. Shematski prikaz okolice difuzorja, ki je bila upoštevana pri numeričnem izračunu tokovnega polja v difuzorju (mere so v milimetrih)

Fig. 9. Schematic view of the diffuser surrounding used for the numerical calculation of the diffuser flow field (all dimensions in millimetres)



Sl. 10. Primerjava vrednosti povprečenih aksialnih hitrosti na izstopu iz difuzorja - koordinatna os x ( $f = 30 \text{ Hz}$ ,  $Re = 1,17 \times 10^4$ )

Fig. 10. Comparison of values of averaged axial velocities at the diffuser outlet – coordinate axis x ( $f = 30 \text{ Hz}$ ,  $Re = 1.17 \times 10^4$ )

Vsi turbulentni modeli napovejo povečanje vzdolžnih komponent hitrosti (sl. 10) tik ob steni vrtečega se difuzorja, kjer te vrednosti dosežejo velikost 1,1 m/s (model  $k-\omega$  SST) do 1,4 m/s (model  $k-\varepsilon$ ), torej so velikostnega razreda izmerjenih vrednosti. Vzdolžne hitrosti se pri preskušu zmanjšajo na vrednost  $\sim 0$  m/s že na oddaljenosti  $r/R = 0,95$ , medtem ko je pri turbulentnih modelih to zmanjšanje bolj položno. Najhitreje se zmanjšajo vrednosti vzdolžne hitrosti pri rezultatih modela Reynoldsovih napetosti, najpočasneje pa pri modelu  $k-\varepsilon$ . Tudi majhno območje povratnega toka, ki se pojavi pri preskušu na oddaljenosti  $r/R \approx 0,92$ , napovedo turbulentni modeli pri nižjih vrednostih  $r/R$  (razen modela  $k-\omega$ , ki povratnega toka na tem delu osi  $x$  ne napove).

Zaradi širšega pasu velikih vrednosti vzdolžnih komponent hitrosti zraka ob steni difuzorja model  $k-\varepsilon$  tudi ne napove dovolj velikih vzdolžnih hitrosti v bližini vzdolžne osi difuzorja. Tu sta eksperimentalnim vrednostim precej bliže ostala dva modela, še posebej model Reynoldsovih napetosti.

### 3 SKLEPI

V prispevku je bila izvedena analiza kinematike toka zraka v vrtečem se vzdolžnem difuzorju s kotom razširitve  $18^\circ$  z namenom ugotoviti vpliv vrteče se stene na tok v difuzorju. Analiza je bila opravljena z meritvami hitrostnega polja z metodo LDA ter z numeričnim modeliranjem toka v difuzorju.

Rezultati so potrdili pojav dveh tipov toka v vrtečem se difuzorju: vrteči se tok zraka ob steni in nevrteči tok v vzdolžni osi difuzorja; to pomeni, da vpliv vrtenja stene ne seže globoko v notranjost difuzorja. Profili obodne komponente hitrosti so zato vbočeni. V območju  $r/R > 0,9$  se pojavi ekstrem vrednosti vseh treh komponent hitrosti, predvsem na tistih prečnih prerezih difuzorja, ki so bliže izstopu. Rezultati preskusa so poleg tega pokazali tudi odvisnost poteka komponent hitrosti zraka v vrtečem se difuzorju od vrtilne frekvence difuzorja in Reynoldsovega števila.

V splošnem so najbližje rezultatom preskusnih meritev rezultati modela Reynoldsovih napetosti, kar potrjujejo tudi rezultati modeliranja toka znotraj vrtečih se cevi [8]. To izhaja iz same narave tega turbulentnega modela, saj upošteva precej manj poenostavitev kot dvoenačbeni modeli. Posledica tega je daljši čas računanja oziroma večji računski napor, ki ga model Reynoldsovih napetosti zahteva.

All three turbulent closure models predict an increase in the axial velocity components (Fig. 10), directly at the rotating diffuser wall, where the axial velocities reach values from 1.1 m/s (model  $k-\omega$  SST) up to 1.4 m/s (model  $k-\varepsilon$ ) – the predicted values are therefore in the region of the measured values. The measured axial velocities during the experiment drop to  $\sim 0$  m/s at a distance of  $r/R = 0.95$ , whereas the drop in the axial velocity values predicted by the turbulent closure models is not so steep. The fastest decrease in the axial velocity values is predicted by the Reynolds stresses model, and the slowest by the  $k-\varepsilon$  model. Apart from that, a small region of the reverse flow, which was observed at a distance  $r/R \approx 0.92$  during the experiment, was predicted at lower values of  $r/R$  by the models (with the exception of the  $k-\omega$  model, which does not predict the reverse flow on this part of the  $x$ -axis).

Because of the broader band of high values of the axial velocity components of the airflow near the diffuser wall the  $k-\varepsilon$  model fails to predict values of the axial velocities that are high enough at the diffuser longitudinal axis; the results of other two models in this region of the diffuser are thus closer to the experimental ones, especially in the case of the Reynolds stresses model.

### 3 CONCLUSIONS

An analysis of the flow kinematics in an axially rotating diffuser with an  $18^\circ$  cone angle was carried out in order to investigate the influence of the rotating diffuser wall on the airflow. This was achieved by the use of an LDA system and by numerical modeling of the airflow inside the diffuser.

The results confirm two general types of flow inside the rotating diffuser: one in the outer rotating region and the second within the inner non-rotating region. This means that the influence of the rotating wall on the airflow does not reach deep inside the diffuser. The tangential velocity profiles are therefore concave. There is a maximum of all three velocity components in the region  $r/R > 0.9$  for the diffuser transverse sections that are close to the diffuser outlet. In addition, the results of the experiment showed the dependence of the distribution of airflow velocity components on the rotating frequency of the diffuser and on the Reynolds number.

The results of the Reynolds' stresses model are generally closest to the results of the experimental measurements, which is also confirmed by the results of the flow modelling inside the rotating straight pipes [8]. This comes from the nature of this turbulent closure model, since the model itself incorporates far fewer simplifications in comparison to the two-equation closure models. The consequence of this is the longer calculation time (greater calculation effort) required by the Reynolds stresses model.

4 LITERATURA  
4 REFERENCES

- [1] Kováts, A. (1964) Design and performance of centrifugal and axial flow pumps and compressors, *Pergamon Press Ltd.*, Oxford.
- [2] Gupta, A. K., D.G. Lilley, N. Syred (1984) Swirl flows, *Abacus Press*, Tunbridge Wells.
- [3] Imao, S. M. Itoh, T. Harada T. (1996) Turbulent characteristics of the flow in an axially rotating pipe, *Int. J. Heat and Fluid Flow*, Vol. 17, No. 5, 444-451.
- [4] Clausen, P. D., S.G. Koh, D.H. Wood (1993) Measurements of a swirling turbulent boundary layer developing in a conical diffuser, *Experimental Thermal and Fluid Science*, 6, 39-48.
- [5] Cannon, J. N., W.M. Kays (1969) Heat transfer to a fluid flowing inside a pipe rotating about its longitudinal axis, *ASME Journal of Heat Transfer*, Vol. 91, No. 1, 135-139.
- [6] Murakami, M., K. Kikuyama (1980) Turbulent flow in axially rotating pipes, *Journal of Fluids Engineering*, Vol. 102, 97-103.
- [7] Schlichting, H., K. Gersten (2000) Boundary-layer theory, *Springer*, Berlin.
- [8] Hirai, S., T. Takagi, M. Matsumoto (1988) Predictions of the laminarization phenomena in an axially rotating pipe flow, *Journal of Fluids Engineering*, Vol. 110, 424-430.

Naslova avtorjev: mag. Tom Bajcar  
prof.dr. Brane Širok  
prof.dr. Ferdinand Trenc  
Fakulteta za strojništvo  
Univerza v Ljubljani  
Aškerčeva 6  
1000 Ljubljana  
tom.bajcar@fs.uni-lj.si  
brane.sirok@fs.uni-lj.si  
ferdinand.trenc@fs.uni-lj.si

dr. Dragica Jošt  
Turboinstitut  
Rovšnikova 7  
1000 Ljubljana  
dragica.jost@turboinstitut.si

Authors' Addresses: Mag. Tom Bajcar  
Prof. Dr. Brane Širok  
Prof. Dr. Ferdinand Trenc  
Faculty of Mechanical Eng.  
University of Ljubljana  
Aškerčeva 6  
1000 Ljubljana, Slovenia  
tom.bajcar@fs.uni-lj.si  
brane.sirok@fs.uni-lj.si  
ferdinand.trenc@fs.uni-lj.si

Dr. Dragica Jošt  
Turboinstitut  
Rovšnikova 7  
1000 Ljubljana, Slovenia  
dragica.jost@turboinstitut.si

Prejeto:  
Received: 20.12.2002

Sprejeto:  
Accepted: 31.1.2003